

Effect of Magnetic Field on Current Collection to a Bare Tether in LEO

Tatsuo Onishi* and Manuel Martínez-Sánchez†

Massachusetts Institute of Technology

Cambridge, Massachusetts, USA

David L. Cooke

Air Force Research Laboratory

Space Vehicle Directorate, Hanscom AFB, MA, USA

Juan R. Sanmartín

ETSI Aeronáuticos

Universidad Politécnica de Madrid, Madrid, Spain

An electrodynamic Tether is a long thin conductive string deployed from a spacecraft. A part of the ED tether near one end, which is rendered positive by the Electromotive force (EMF) along the tether, collects electrons from the ambient plasma. In the frame of reference moving with the tether, ions flow toward the tether, get deflected near the tether by its high positive potential and create a wake. Due to the asymmetry of plasma distribution and the weak but significant Geomagnetic field, the conventional probe theory becomes almost inapplicable. Computational work for the prediction of current collection is thus necessitated. In this paper, we analyze effects of magnetic field on velocity distribution function at a point that is far from the tether, and discuss a new way to treat electrons at computational boundary. Three cases with different magnetic field are simulated and compiled so as to provide a part of the pre-flight prediction of the space experiment by NASA ProSEDS, which is planned September 2002. Plasma oscillations and associated increased electron density due to trapped electrons are recognized in the computation when the magnetic field is absent. In the presence of magnetic field, current collections tend to be 2 ~ 3 higher than the 2D Orbital-Motion-Limit (OML) without significant appearance of trapped electrons. It is argued that, because of the three-dimensional motions of electrons, the 3D OML limit may be the upper limit even though the geometry is two-dimensional.

Introduction

An electrodynamic (ED) bare tether has been considered as an alternative method of propulsion without expenditure of propellant. One of the difficulties ED tether engineers are confronted with is the estimation of current-voltage characteristics. The analysis is quite complicated because of the small but significant geomagnetic field and the spacecraft's relative motion to both ions and electrons [2] [3]. One of the approaches to this solution is the use of a particle-dynamics numerical method. In the numerical analysis of space plasma, one of the most reliable approaches has been the Particle-In-Cell (PIC) method. In this paper we apply a PIC code for a two dimensional collisionless plasma under the effects of magnetic field and the spacecraft's relative motion.

In predicting the electron current collection to a bare electrodynamic tether, the 2D OML current is often used as an upper limit under steady plasma

condition. For a geometrically 2D problem defined in x-y plane, such as a bare tether, OML current, "2D" or "3D", is calculated by considering electron motions only in the plane perpendicular to the tether (x-y plane). In this paper, a cylindrical bare tether is aligned with z-axis, magnetic field is given by $\vec{B} = (0, -B, 0)$ and plasma flow by $\vec{U} = (U, 0, 0)$. Electrons which can travel from infinity to the tether surface *only in the x-y plane* are counted as the contribution to the current.

When computing the current by counting the electron flux on the collecting surface, electrons which have an energy less than the potential difference between this surface and infinity are excluded. In a geometrically 2D surface and with no magnetic field, some hypothetical electrons may be additionally excluded, because, even though their energy is sufficient, it resides mainly in the component parallel to the object's axis, and there is no mechanism to transfer it to the perpendicular plane; if the perpendicular part of the energy is less than the potential difference, these electrons can not exist near the surface.

For the same 2D object, but with some magnetic

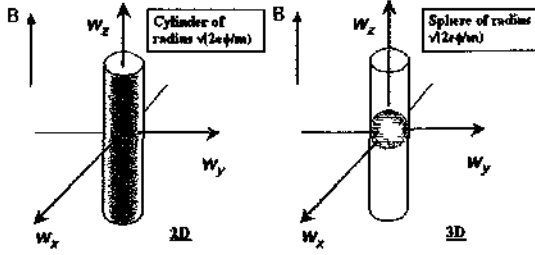


Figure 1: Electrons in velocity space. Electrons with velocities inside indicated regions, cylinder (2D,left) and sphere (3D,right), are excluded in the calculation of the OML current.

field perpendicular to it, gyrations cyclically convert motion along the object's axis to motion perpendicular to it. Whether or not an electron with sufficient total energy but insufficient perpendicular energy can be found near the surface is a complicated question. Considering a reversed trajectory, starting from the surface, the answer depends on whether or not the magnetic rotation is rapid enough to direct the electron away from the object before the electrostatic attraction forces it back to it.

Now away from the surface in the presheath, where there is no such object and a local potential is not so large that the electrostatic attraction is negligible or comparable with the magnetic effect. All electrons with sufficient total energy can be traced back their trajectories to infinity.

In following sections, we elaborate on the above-mentioned 3D OML theory to the current collection to a bare cylindrical tether in the presence of magnetic field. We incorporate the condition at the computational boundary. We show some results from several simulations with different plasma parameters. Finally we discuss the effects of magnetic field on the current collection to a cylindrical bare tether.

2D vs. 3D OML theory

Let us go briefly through the derivation of OML current to a positively biased cylindrical bare tether both in 2D and 3D. For brevity, we assume Maxwellian distribution at infinity where potential is set to zero, $\phi = 0$. And we also neglect multiple intersections of an electron trajectory by the tether. Thus we consider all electrons only in terms of its total energy and total perpendicular energy

(Laframboise-Parker [6]).

In both 2D and 3D cases, the calculation of current is performed by counting all electrons entering into the surface of a tether, whose trajectories can be traced back to infinity. When dealing with a geometrically two-dimensional problem such as a cylindrical bare tether, the "infinity" has to be that of x-y plane perpendicular to the tether.

The 2D OML current is derived as follows; on the surface of the tether of potential ϕ_p , the one-side flux is calculated by taking the first moment of the electron distribution. In taking the integral over velocity space, all electrons whose trajectory can be traced back to infinity of x-y plane are counted. These electrons have enough total energy and can originate from infinity. They are characterized by having a velocity

$$v_x^2 + v_y^2 \geq 2e\phi_p/m. \quad (1)$$

In the direction parallel to the tether (z-direction), there is no electric field. Therefore v_z is constant and can have any value. In velocity space, these electrons reside inside a cylinder of radius $\sqrt{2e\phi_p/m}$ as shown in Figure 1. The current density is then obtained as

$$\begin{aligned} j_{OML}(2D) &= \iiint_{v_x^2+v_y^2 \geq 2e\phi_p/m, v_z > 0} ev_{\perp} f_e dv \\ &= e \int_{-\infty}^{\infty} dv_z \int_{\sqrt{2e\phi_p/m_e}}^{\infty} \int_{-\pi/2}^{\pi/2} v_{\perp} f_e v_{\perp} \cos\theta d\theta dv_{\perp} \\ &= \frac{en_{\infty}\bar{c}_{\infty}}{2\sqrt{\pi}} \left[\sqrt{\frac{e\phi_p}{kT_{\infty}}} + \frac{\sqrt{\pi}}{2} e^{\frac{e\phi_p}{kT_{\infty}}} \operatorname{erfc} \left(\sqrt{\frac{e\phi_p}{kT_{\infty}}} \right) \right] \\ &\rightarrow \frac{en_{\infty}\bar{c}_{\infty}}{2\sqrt{\pi}} \sqrt{\frac{e\phi_p}{kT_{\infty}}} \end{aligned} \quad (2)$$

since, in the limiting form, $x \rightarrow \infty$, we have

$$\operatorname{erfc}(x) = 1 - \operatorname{erf}(x) = \frac{1}{\sqrt{\pi}} \int_x^{\infty} e^{-t^2} dt \quad (3)$$

$$\rightarrow \frac{2}{\sqrt{\pi}} \frac{e^{-x^2}}{x} \quad (4)$$

where \bar{c}_{∞} is the random thermal velocity given as

$$\bar{c}_{\infty} = \sqrt{\frac{8kT_{\infty}}{\pi m_e}} \quad (5)$$

Therefore, when $\frac{|q\phi|}{kT_{\infty}} \gg 1$, the 2D OML current density is given as

$$j_{OML}(2D) = \frac{en_{\infty}}{\pi} \sqrt{\frac{2e\phi_p}{m_e}} \quad (6)$$

Next, let us consider the 3D OML current to a cylindrical tether in the presence of magnetic field. As in the 2D case, all electrons at a point of the

tether surface whose trajectory can be traced back to infinity of x-y plane should be counted in the calculation of the current. These electrons are characterized by

$$v_x^2 + v_y^2 + v_z^2 \geq 2e\phi_p/m_e. \quad (7)$$

Then the current density is then obtained as

$$\begin{aligned} j_{OML}(3D) &= \iiint_{v_x^2+v_y^2+v_z^2 \geq 2e\phi_p/m_e, v_\perp > 0} ev_\perp f_e dv \\ &= en_\infty \sqrt{\frac{\kappa T_e}{2\pi m_e}} \left(1 + \frac{e\phi_p}{\kappa T_e} \right) \end{aligned} \quad (8)$$

Equation (8) shows much higher current density in a magnetized case than in an unmagnetized case.

As shown above, even if the geometry of the problem is two-dimensional, we can expect the 3D OML current as the upper limit in a steady state. However, this analysis does not guarantee a much higher current collection than the 2D OML current to a bare cylindrical tether, because of the presence of electron trajectories which may intersect with the tether multiple times.

We can still expect higher current collection than the 2D OML current to a bare cylindrical tether in LEO. We applied this analysis at the computational boundary where the local potential is positive (except in a wake) and magnetic effect is strong enough to apply the 3D OML theory. In the following section, we show the computation of our code with the treatment of the boundary condition, based on the 3D OML theory.

Computation

The Particle-In-Cell (PIC) method is used for the calculation of current collection to a bare cylindrical tether with and without magnetic field. We run a nominal case specified by plasma parameters given in Table 1. Two other cases with $B = 0(G)$ and $B = 0.6(G)$ are examined to see the effects of magnetic field on the current calculation.

Quasi-neutrality Condition

The quasi-neutrality condition is applied at each outside boundary point by equating the electric charge density of outgoing particles and incoming particles to zero as,

$$n_i^{out} - n_e^{out} = n_e^{in}(\phi_b) - n_i^{in}(\phi_b) \quad (9)$$

from which the local potential ϕ_b is solved. Densities of outgoing particles, n_i^{out} , n_e^{out} , in the left hand side are numerically calculated [5]. Densities of incoming particles in the right hand side are given as an analytical function of a local boundary potential

Density	$n_\infty = 10^{11}(1/m^3)$
Magnetic field	$B = 0.3 (G)$
Tether potential	$\phi_p = 25 (eV)$
Tether radius Debyelenght	$\frac{d}{d_D} = 1$
Ion mass (O^+)	$M_i = 2.67 \times 10^{-27} (kg)$
Satellite speed	$U = 8 (km/sec)$
Electron Temperature	$T_e = 0.1 (eV)$
Ion Temperature	$T_i = 0.1 (eV)$
Debye length	$d_D = 0.74 \times 10^{-2} (m)$
Larmor radius	$r_L = 0.25 \times 10^{-1} (m)$
Angle of the tether to its motion	$\theta = 90 (deg)$

Table 1: Plasma parameters for the nominal case

ϕ_b . Following the argument given in the previous section, we calculate incoming electron density at a boundary point of positive potential ϕ_b separately for $B = 0$ and for $B \neq 0$. Since the local boundary potential is typically positive (except for a wake) but small, magnetic effects in the $B \neq 0$ case are still strong. And there is no object such as a tether with which a gyrating electron intersect. Therefore we can apply the argument at the boundary point, if not on the surface of a tether. Incoming electron densities can be written as

$$n_e^{in}(\phi_b, B = 0) = \iiint_{v_x^2+v_y^2+v_z^2 \geq 2e\phi_b/m_e, v_\perp > 0} f_e dv \quad (10)$$

$$n_e^{in}(\phi_b, B \neq 0) = \iiint_{v_x^2+v_y^2+v_z^2 \geq 2e\phi_b/m_e, v_\perp > 0} f_e dv \quad (11)$$

where the electron velocity distribution at the boundary, f_e , is given as

$$f_e = N_\infty \exp\left(-\frac{(v_x - U)^2 + v_y^2 + v_z^2}{v_{Te}^2} + \frac{e\phi_b}{\kappa T_e}\right) \quad (12)$$

and $N_\infty = n_\infty \left(\frac{m_e}{2\pi\kappa T_e}\right)^{3/2}$ is a normalization factor. v_\perp is the normal component of incoming velocity to a boundary surface. Equations (10) and (11) are plotted in Figure ???. As the 2D OML theory claims, the incoming electron density for $B = 0$ does not increase as the local potential increases.

The number of particles to inject into the computational domain at each boundary point is calculated from the incoming flux of particles. Likewise, incoming electron fluxes are also computed at a local boundary point separately for $B = 0$ and $B \neq 0$. The formula for the calculation is the same as that used above for the calculation of the OML current, equations (2) and (8). We merely need to replace the tether potential ϕ_p with ϕ_b and include



Figure 2: Incoming electron density as a function of a local potential ϕ . In two-dimensional case (left), electron density decreases a little bit due to the flowing effects. In three-dimensional case (right), electron density increases as a local potential increases.

a plasma flow velocity (tether velocity) U in a distribution function f_e . That is, we use f_e given by (12), but not the Maxwellian distribution.

Results

Nominal Case

The nominal case is defined in Table 1. We use this case as a starting point and change the magnetic field for other cases.

In Figure 4 we show instantaneous distributions of field quantities. From top left in the clockwise direction, trapped electron density, non-trapped electron density, ion density, potential, electric charge density and electron density are shown. Electron and ion densities are normalized by that at infinity. Electric charge density is normalized by en_∞ . Potential is in actual units (eV).

The ion density distribution shows strong effects of the mesothermal condition. First, a wake region behind the tether is noticed. The wake is created by the quasi one-dimensional motion of massive ions. Ions are flowing toward the tether from the left (ram region) almost one-dimensionally. Due to the tether's large potential, ions are slowed down in the ram region and deflected from the 1-D trajectory. Because of this slow-down, ions increase their density. The peak of increased density reaches 2 ~ 3 times that at infinity. The potential at the peak point corresponds to the ion ram energy (5eV). Because of the slightly positive potential in the presheath region, ion density is always more than at infinity in the ram region.

In the mesothermal condition, electrons are moving much faster than the tether, therefore the effect of plasma flow is almost negligible. A decisive factor to determine the electron density distribution is the ion density distribution, since a plasma has a strong tendency to maintain the quasi-neutrality in the larger scale than Debye length. This explains

the low density in the wake region. Electron density in the wake region is decreased such that the local Debye length is comparable with the characteristic length of the wake. In this case, the length in the y -direction should be taken as a characteristic length. When electrons are close to the tether, the tether's large potential creates a sheath region where the plasma does not maintain quasi-neutrality. Naturally the size of the sheath is of the order of a few Debye lengths. In Figure 4, the sheath region is clearly presented. A significant electron population ($n_e \geq n_\infty$) is recognized around the tether. The region extends up to 10 Debye lengths (The radius of the tether is 1 Debye length).

At the left bottom of Figure 4, the net electric charge density is plotted. Since the size of the computational domain was chosen in such a way that it contains a sheath region, quasi-neutrality can be seen in the presheath region. There are, however, three zones where the quasi-neutrality does not prevail. The first one is the wake. As the electron density is very low due to the ion depletion, the local Debye length is so large that the quasi-neutrality does not hold. Second is the sheath in the vicinity of the tether where a large potential due to the tether bias prohibits the ion population and attracted electrons form a non-neutral sheath. The last, less strong, is due to the ion density caustic line ahead of the tether. Ions are slowed down as they climb up the potential hill toward the tether. Decelerated ions increase in density and the density reaches its peak at a point of potential equal to 5eV, which is the ion ram energy. In order to maintain the quasi-neutrality, plasma tends to gather more electrons near the peak. In front of the tether, increased ion density is neutralized by the electrons carried through the potential wing. However the quasi-neutralization is not complete at the sides of the tether.

At the right bottom, the electric potential is plotted. As mentioned above, most of presheath has a positive potential. Behind the tether there is a wake where negative potential prevails. Along the magnetic field near the tether, there are potential wings which have higher potential than other parts of presheath. Due to the magnetic field, electrons gyrate and can not transport themselves across the magnetic field. Therefore except for very few electrons with a large velocity in the ram side, most of electrons are brought in along the magnetic field lines. Thus, plasma extends potential wings along the magnetic field to attract enough electrons to gain the quasi-neutrality. In front of the tether and the wing, the potential is almost as low as potential at infinity ($\phi_0 = 0$), showing little influence of the tether presence.

Any significant plasma oscillation is not observed in this case. However, along the magnetic field

lines near the tether where ions increase in density, trapped electrons are observed. Moreover in the sheath near the tether, there is a significant population of trapped electrons.

Finally for this nominal case, the current collected is 2 ~ 3 times larger than the 2D OML current, but much lower than the 3D OML current which would be $J_{OML}(3D)/J_{OML}(2D) = \left(1 + \frac{e\phi_p}{\kappa T_e}\right) / \left(\frac{2}{\sqrt{\pi}} \sqrt{\frac{e\phi_p}{\kappa T_e}}\right) = \frac{\sqrt{\pi}}{2} \sqrt{\frac{e\phi_p}{\kappa T_e}}$ times larger than the 2D OML current. For $\phi_p = 25(eV)$, this rate would be ~ 14.01 .

Case 1 : $B = 0(G)$

In Figure 5, the case with no magnetic field is shown. The effects of magnetic field are very distinct. The absence of magnetic field renders the electron motion totally two dimensional due to the absence of gyration motion. In order for the plasma to maintain the quasi-neutrality, it increases potential so that it can attract more electrons. However, as discussed in the earlier section, in a totally two-dimensional case, higher potential does not increase electron density. But still ion density increases due to the strong tether stopping potential. This creates a region where ion density is higher than electron density. It violates the Bohm stability criterion, which states that, for stability of the sheath formation, the sign of net charge everywhere in the presheath and the sheath must be the opposite to that of the probe potential. The deficit electrons need to be supplied by extra electrons which need to be present as a result of plasma oscillations. In order to keep those trapped electrons confined in the presheath, the plasma potential stays positive enough that trapped electrons have a negative total energy, $\frac{1}{2}m_e(v_x^2 + v_y^2) - e\phi < 0$, and can not escape to infinity where $\phi = 0$.

Next thing to realize in the $B = 0(G)$ case is the spreading of potential into the ram region. Unlike a magnetized case, electrons can be brought in from all directions. Accordingly, the potential wings disappear.

Trapped electrons are observed where the ion caustic line is found. As seen from the net charge (bottom left), electron population along the caustic line is not enough to maintain quasi-neutrality. Therefore the Bohm stability criterion is not yet satisfied.

The current collection is about 1.2 ~ 1.5 times the 2D OML current. Strong plasma oscillation is observed at about 0.2 times plasma frequency of the undisturbed plasma (Figure 3).

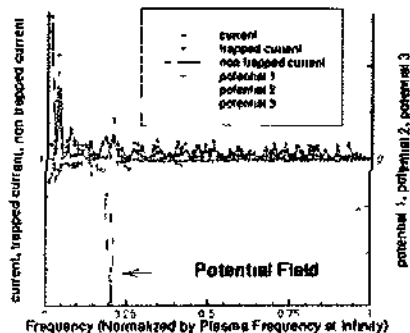


Figure 3. FFT analysis of current collection and local potentials. Both current collection and local potentials have characteristic frequency at $\omega \sim 0.2 \times \omega_p$

Case 2 : $B = 0.6(G)$

In Figure 6 The larger magnetic field decreases the gyro-radius of particles. The gyroradius of ions is still large compared to the characteristic length of the problem so that we can still ignore their gyration effects. On the other hand, the electron gyroradius is comparable to the size of the tether cross-section and its effect on the plasma behavior is recognizable. Smaller electron gyroradius makes the "magnetic wing" narrower than in the nominal case. Since the magnetic wing is the source of electrons for the maintenance of quasi-neutrality near the tether where ions increase their density, the plasma potential in the magnetic wing becomes relatively higher in order to attract more electrons. The increased potential in the magnetic wing also affects the ion trajectories.

Trapped electron is observed ahead of the tether where the increased ion density is found. Like the nominal case, the plasma oscillation is not observed. Current collection is found to be twice as much as the 2D OML current.

Conclusion

The application of the 3D OML theory to the calculation of current collection to a bare cylindrical

tether is extended to study magnetic field effects. While it still does not guarantee the 3D OML current to the tether, it proves higher current collection than the 2D OML current even in the steady state. In our computation, the 3D OML theory is applied at the computational boundary points where the local potential is positive but not very large.

A few simulations are performed with different magnetic field, $B = 0, 0.3$ and $0.6(G)$. In the unmagnetized case, because of the deficit electrons due to the 2D OML theory, plasma becomes oscillatory and traps electrons. Having a negative total energy, these trapped electrons can not escape to infinity and are confined in the presheath. This makes up for the deficit of electron density and marginally satisfies the Bohm stability criterion. In the computation, a typical frequency is recognized to be around 0.2 times the plasma frequency of the unperturbed plasma.

In both magnetized cases, in the presheath, electron's motion follows the 3D OML theory, meaning that all electrons with sufficient total energy are counted. The increased ion density by the high tether potential is matched by the electron density increased by a locally increased potential. A region where ion density is higher than electron density as in the unmagnetized case is not recognized.

The current collection to a bare cylindrical tether is typically 2 ~ 3 times more than the 2D OML theory in the presence of magnetic field. In the limit of $B \rightarrow 0$, as long as $B \neq 0$, magnetic effect brings in more electrons than prescribed by the 2D OML theory under the totally collisionless state. However, in the computation, in the limit of $B \rightarrow 0$, the outside boundary needs to be taken far enough for magnetic effect to be comparable with or stronger than the electrostatic force by the tether.

Acknowledgments

This work was supported through a grant from the AFOSR (Technical monitor: Kent Miller).

References

- [1] Chung, P.M., L. Talbot and K.J. Touryan, *Electric Probes in Stationary and Flowing Plasmas; Theory and Application*, Springer-Verlag, 1975
- [2] Cooke, D.L. and I.Katz, *TSS-1R electron currents: Magnetic limited collection from a heated presheath*, Geophys. Res. Lett., Vol. 25, No.5, Page753-756, March 1, 1998
- [3] Laframboise, J. G., Current collection by a positively charged spacecraft: Effects of its presheath, *Journal of geophysical research*,102(2A), February 1997.
- [4] Onishi, T., *Electron Current Collection by a Positively Charged Tether, Using a Particle-In-Cell Method*. Master's Thesis, MIT (Aeronautics/Astronautics) May 1998
- [5] Onishi, T., M. Martinez-Sanchez and D.L. Cooke *Computation of Current to a Moving Bare Tether*, AIAA2000-3865 ,2000
- [6] Laframboise, J.G. and L.W. Parker, Probe design for orbit-limited current collection. *Phys. Fluids*, page629, Vol 16, Num 5, May 1973.
- [7] Birdsall, C. K. and Langdon, A. B., *Plasma physics via Computer Simulation*. McGraw-Hill, New York. 1985.
- [8] Seldner, D. and Westermann, T., Algorithms for interpolation and localization in irregular 2D meshes. *Journal of Computational Physics*, 79, pp1-11, 1988.
- [9] Wang, J., Liewer, P.C., Karmesin S. R. and Kondrashov, D., 3-D deformable grid electromagnetic Particle-In-Cell for parallel computers. *AIAA 97-0965*, 1997.
- [10] Laframboise, J. G., Theory of spherical and cylindrical langmuir probe in a collisionless, maxwellian plasma at rest. Technical Report 100, University of Toronto, Institute of Aerospace Studies Report, 1966.
- [11] Langmuir, S. and Mott-Smith, H. M., The theory of collection in gaseous discharge. *Physical Review*, 28, October 1926.
- [12] Goldstein, H. *Classical Mechanics*. Addison-Wesley Pub. Co., Massachusetts, 1980.

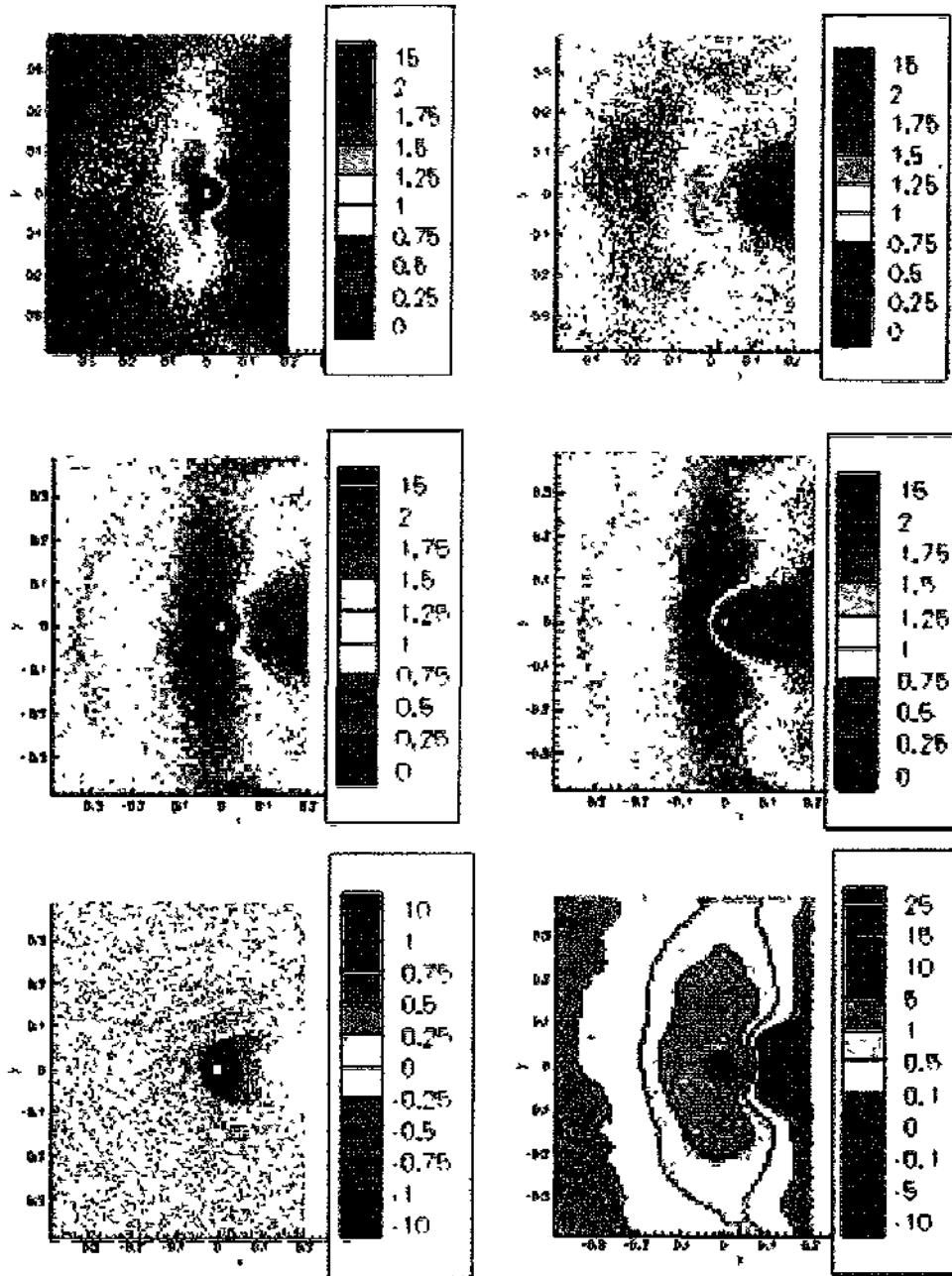


Figure 4: Instantaneous maps of the nominal case ($B = 0.3(G)$). Trapped electron density (top left), non-trapped electron density (top right), total electron density (middle left), ion density (middle right), net charge density (bottom left) and electric potential (bottom right). All densities are normalized by that of unperturbed plasma, n_{∞} , net charge by en_{∞} and electric potential is in the actual unit (eV)

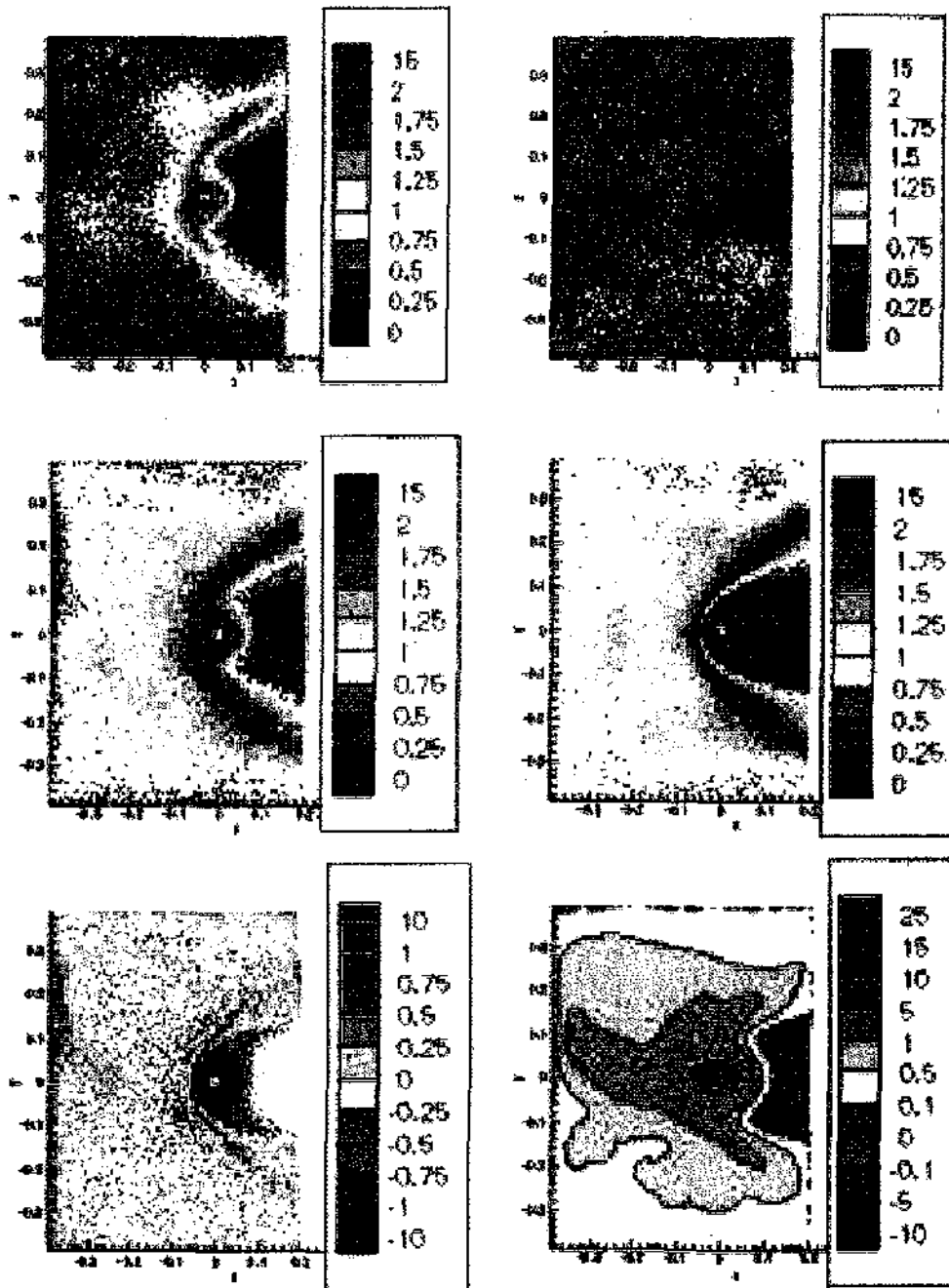


Figure 5: Instantaneous maps of an unmagnetized case ($B = 0(G)$). Trapped electron density (top left), non-trapped electron density (top right), total electron density (middle left), ion density (middle right), net charge density (bottom left) and electric potential (bottom right). All densities are normalized by that of unperturbed plasma, n_{∞} , net charge by en_{∞} and electric potential is in the actual unit (eV)

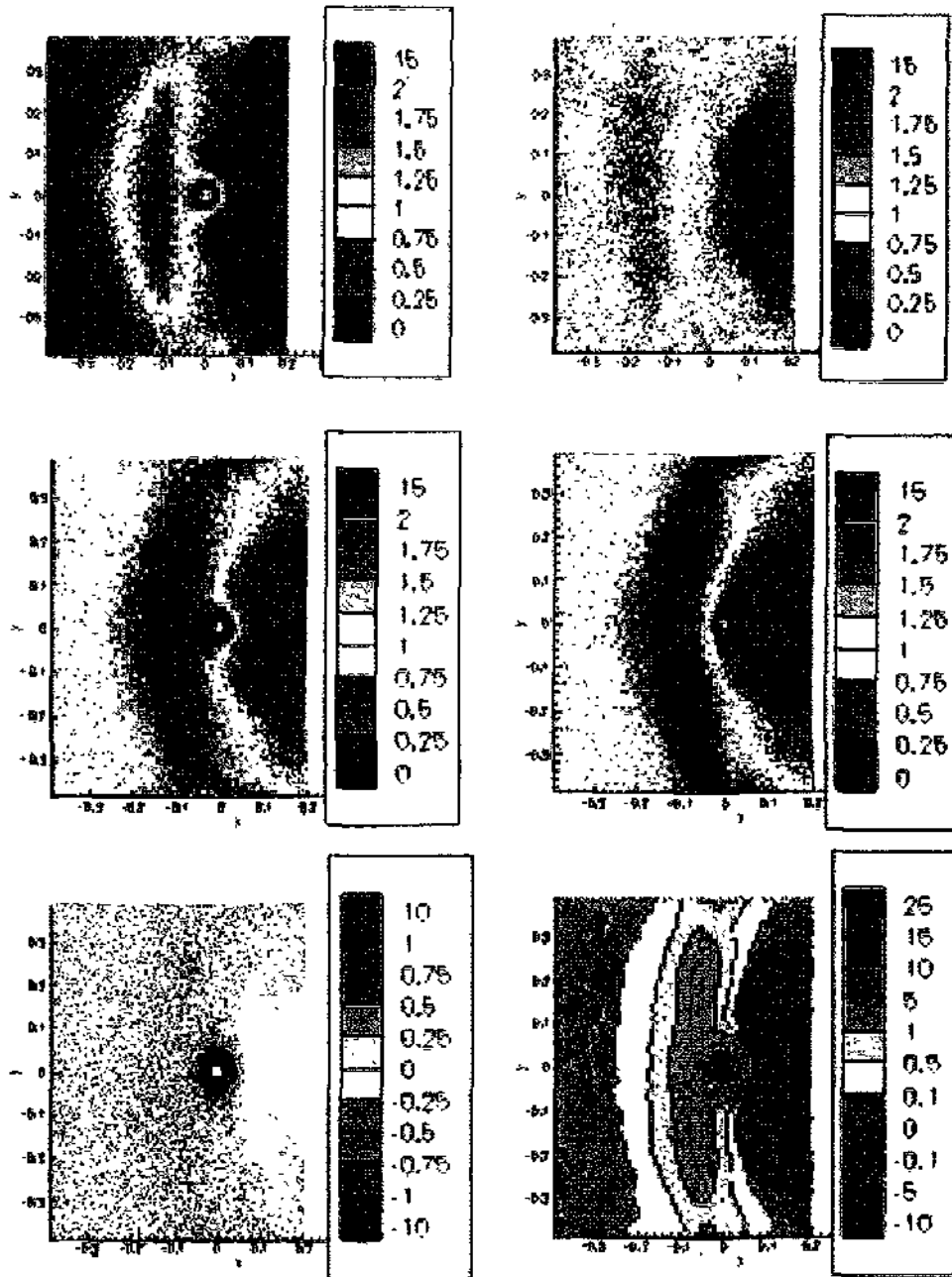


Figure 6: Instantaneous maps of a stronger magnetic case ($B = 0.6(G)$). Trapped electron density (top left), non-trapped electron density (top right), total electron density (middle left), ion density (middle right), net charge density (bottom left) and electric potential (bottom right). All densities are normalized by that of unperturbed plasma, n_{∞} , net charge by en_{∞} and electric potential is in the actual unit (eV)